JOURNAL OF GEOPHYSICAL RESEARCH, VOL. 88, NO. A4, PAGES 3079–3093, APRIL 1, 1983

Electrostatic Bursts Generated by Electrons in Landau Resonance With Whistler Mode Chorus

LEE A. REINLEITNER, DONALD A. GURNETT, AND TIMOTHY E. EASTMAN

Department of Physics and Astronomy, The University of Iowa, Iowa City, Iowa 52242

Recent studies of wideband plasma wave data from the ISEE 1 and ISEE 2 spacecraft have revealed that whistler mode chorus emissions in the earth's outer magnetosphere are often accompanied by high-frequency bursts of electrostatic waves with a frequency slightly below the electron plasma frequency. Investigations have shown that in some cases the electrostatic waves are modulated at the chorus frequency. Further studies using the plasma analyzer (LEPEDEA) data on ISEE 1 indicate that these bursts are produced by a 'beam' of electrons in Landau (longitudinal) resonance with the chorus wave and thus moving at the chorus phase velocity. A threshold exists in the chorus intensity below which the electrostatic bursts do not appear. The high-frequency electrostatic waves are believed to be caused by a type of two-stream instability called the resistive medium instability. The resistive medium instability is characterized by a reduction in the electrostatic burst frequency below the electron plasma frequency, The instability is applicable only in the regime where V_0/V_T is on the order of 1, where V_0 is the velocity of the beam and V_T is the average thermal velocity of the plasma electrons. Our derivation assumes cold ions but warm electrons. The instability requires Landau damping to operate. Thus the beam velocity must be in the region of steep slope on the electron distribution function rather than in the high-velocity tail region. In the cases examined from the LEPEDEA data the electron thermal energies are on the order of a few hundred eV. The beam velocities in the observed cases were $\approx$400 eV and $\approx$630 eV, thus verifying that the electrostatic bursts are in the proper regime for the resistive medium instability.

1. INTRODUCTION

The earth's magnetosphere has proven to be a rich source of various types of plasma wave modes. This study treats a new type of electrostatic wave that appears as very sharply defined bursts and is closely correlated with a type of electromagnetic whistler mode wave known as chorus. These waves occur in the outer magnetosphere, just inside the magnetospheric boundary layer, on the dayside region of the magnetosphere.

Chorus is a type of low-frequency electromagnetic emission that is believed to result from a cyclotron resonance interaction with energetic electrons in the outer magnetosphere. The frequency range of the chorus emissions associated with the electrostatic bursts is approximately 100–800 Hz. Dayside chorus usually has a discrete frequency-time structure, consisting of narrowband tones increasing in frequency with increasing time [*Helliwell*, 1965]. Chorus also occurs as a simple banded emission with little or no structure [*Burtis and Helliwell*, 1969].

On the dayside of the earth, chorus waves are generated by electrons with energies in the range of 5–150 keV [*Burton and Holzer*, 1974]. The generation mechanism is believed to be a Doppler-shifted cyclotron resonance with these high-energy electrons near the equatorial plane [*Dowden*, 1962; *Brice*, 1964; *Helliwell*, 1967]. The general resonance condition for a wave of frequency ω interacting with an electron moving in a magnetic field is

$$k_{\|} v_{\|} = \omega - m|\omega_{ge}| \tag{1}$$

where $m = 0, 1, 2, \ldots$ are integers, $v_{\|}$ and $k_{\|}$ are velocity and wave vector components parallel to the magnetic field, and ω_{ge} is the electron gyrofrequency.

For cyclotron resonance, the integer m must be nonzero. The special case where m is zero is called the Landau resonance. *Kennel and Petschek* [1966] showed that the whistler mode is unstable if a sufficiently large positive pitch angle anisotropy exists in the electron distribution function at the resonance velocity. In the earth's magnetosphere a positive pitch angle anisotropy is produced by the atmospheric loss cone in the trapped electron distribution. The whistler mode is unstable whenever the anisotropy exceeds a critical anisotropy. Electrons resonating with the wave are always scattered toward the loss cone by the cyclotron resonance interaction, thereby causing the particles to be precipitated into the atmosphere. Precipitating electrons have been reported in association with chorus emissions [*Oliven and Gurnett*, 1968; *Rosenberg et al.*, 1971] and are believed to be pitch angle scattered by these waves.

Chorus has been known for many years [*Helliwell*, 1965] to be propagating in the whistler mode. For the parameters found in this study, the chorus phase velocity was typically on the order of 1/10 to 1/20 of the speed of light. Although the ray path of the chorus wave tends to follow the ambient field line, the wave vector can be at a substantial angle θ to the field line [*Kennel and Thorne*, 1967; *Burton and Holzer*, 1974; *Burtis and Helliwell*, 1976]. The wave normal angle is not certain due to lack of wave normal measurements in the region of interest, but is generally believed to be in the range from about 0° to 30° (B. T. Tsurutani, private communication, 1982). This relates well to the reported wave normal distribution peak at between 10° and 20° reported by *Burton and Holzer* [1974] for the dayside region with latitude $0° < |\lambda_m| < 25°$.

The electrostatic bursts analyzed in this paper have a frequency much greater than that of the chorus. The frequency is usually somewhat lower than the electron plasma frequency and is normally in the range from about 3 kHz up to 10 kHz. As will be shown, the electrostatic bursts are longitudinal electrostatic waves with wave vectors aligned almost exactly along the ambient magnetic field. In some cases, the amplitude of the electrostatic bursts is shown to have a modulation at the chorus frequency. This modulation is indicative of a strong physical interaction between these two wave modes.

This paper details the investigation of this interaction and

Paper number 2A1984.
0148-0227/83/002A-1984$05.00

provides strong evidence that the electrons responsible for the electrostatic bursts are trapped and accelerated by a Landau resonance interaction with the chorus wave. The primary data used in this work was obtained from the ISEE 1 and ISEE 2 (International Sun-Earth Explorer) spacecraft, which were launched into earth orbit simultaneously on October 22, 1977. These spacecraft were in nearly identical orbits with apogee and perigee geocentric radial distances of 22.5 R_E and 1.12 R_E [*Anderson et al.*, 1981]. The plasma wave data used were obtained from the University of Iowa plasma wave experiment and the instrumentation is described in detail by *Gurnett et al.* [1978]. All of the electric field data taken on the ISEE 1 spacecraft for this work used the 215 m electric dipole antenna. The electric dipole antenna on ISEE 2 has a length of 30 m tip to tip.

High time resolution spectrum measurements were available on ISEE 1 from a 20-channel electric spectrum analyzer which covered a range from 5.62 Hz to 311 kHz, as well as extensive frequency time measurement using the wideband instrumentation. The wideband receiver was used in a mode with two frequency channels for all of this work. One channel extended from 650 Hz to 10 kHz and was transmitted by directly modulating the wideband transmitter output. The other channel extended from 10 Hz to 1 kHz and was transmitted by using an FM subcarrier. Due to the large dynamic range the wideband receiver was provided with an automatic gain control (AGC) which maintained a nearly constant signal amplitude.

Valuable data on the electron velocity distribution function were obtained from the University of Iowa Quadrispherical LEPEDEA (low energy proton and electron differential energy analyzer) instrument on ISEE 1. Full descriptions of the LEPEDEA instrument are given by *Frank et al.* [1978*a*, *b*]. The LEPEDEA instrument samples ion and electron velocity distributions over approximately 98% of the unit sphere. This coverage is obtained by seven pairs of sensors that are used to segment the 162° polar angle range into seven contiguous fields of view. One of the primary LEPEDEA data formats is in the form of E-ϕ spectrograms. This data format is explained in detail in *Eastman and Frank* [1982].

2. Characteristics of the Electrostatic Bursts and Their Relationship to Whistler Mode Chorus

This section is devoted to a description of the electrostatic bursts observed and their relationship to the whistler mode chorus emissions accompanying them. A preliminary study of these relationships has been published by *Reinleitner et al.* [1982]. Figure 1 indicates some of the general features of this phenomenon. The top panel shows a chorus band at about 150–200 Hz, of the type that is often observed in the outer magnetosphere on the dayside of the earth. The chorus frequency is rather low because of the low magnetic field strength in the outer part of the magnetosphere. The discrete features in Figure 1 are a general class of emissions called 'hooks' by *Helliwell* [1965]. In this case the emissions only have rising frequencies, but hooklike features with both descending and then rising frequencies are often observed [*Reinleitner et al.*, 1982].

The features referred to as electrostatic bursts (or simply bursts) are illustrated in the lower panel of Figure 1. These bursts extend in a fairly broad band from about 3 kHz to about 7 kHz and turn on and off very abruptly (on the order of 10 ms). In this case, the electrostatic bursts appear to be strongly correlated to discrete features in the chorus band.

Two particular types of electrostatic bursts occur, both related to chorus. The first type is shown in Figure 1 where the bursts are of short duration, usually less than 1 s. This type of burst is usually correlated with a hooklike feature in the chorus band. The second type is of longer duration and is associated with an intensification of the chorus band rather than a hooklike feature. This type of burst is illustrated in Figure 2. The intensification of the chorus band in this figure is a real feature as determined by the spectrum analyzer data and not simply a AGC effect. The rather abrupt onset and termination of the electrostatic bursts in association with the chorus band intensification indicates that some type of threshold effect is present. Long duration bursts are observed to extend from about 10 s to several minutes. The long duration type of electrostatic bursts

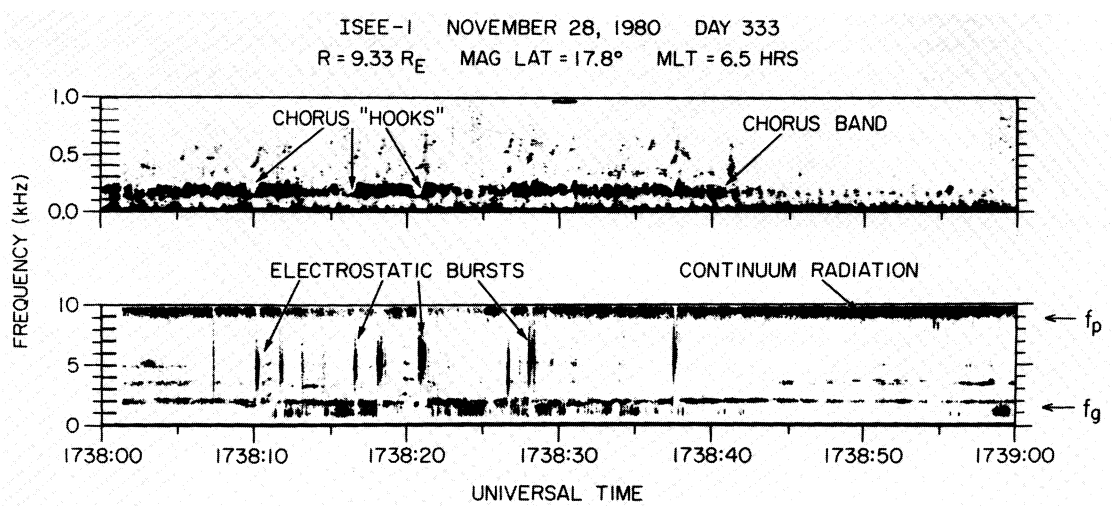

Fig. 1. ISEE 1 frequency-time wideband data illustrating the main characteristics of the electrostatic bursts and their relationship to whistler mode chorus waves. In this case, the electrostatic bursts are correlated to the discrete 'hooks' in the chorus band. The bursts have a much higher frequency range than the chorus and a wider frequency spread. The plasma frequency and the electron gyrofrequency are indicated at the right. The lower edge of the continuum radiation is used to determine the plasma frequency. The time interval covered is one minute.

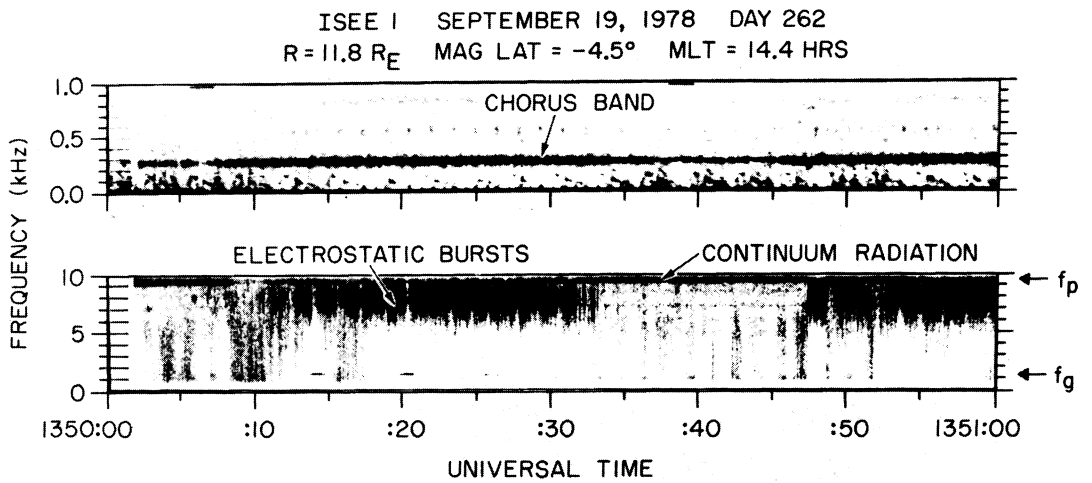

Fig. 2. ISEE 1 frequency-time wideband data illustrating the main characteristics of the long time duration electrostatic bursts when they are correlated with an intensification of the chorus band, but no single discrete chorus feature. The time interval covered is one minute.

are much more commonly observed than the type associated with the discrete hooklike features by roughly a factor of 5 to 10.

A comprehensive survey of the locations where the bursts can be observed has not yet been performed. However, all cases observed so far have been located in the earth's outer magnetosphere near the dayside magnetospheric boundary at about 9–12 R_E. Cases have been found on the dayside region for magnetic local times ranging from 7.0 to 17.5 MLT. All cases observed have been within 30° of the magnetic equator; however, this limitation is probably due to the equatorial nature of the ISEE satellite orbit. Examination of the LEPEDEA data has shown that most of the observed cases are located inward from the magnetospheric boundary layer. Only a few are actually located in the boundary layer region itself. It should be noted that in regions closer to the earth, the plasma frequency tends to go above 10 kHz, which would produce electrostatic bursts at frequencies too high to be observed in the primary mode of operation of the ISEE instrumentation. Thus the general limitations on the locations of the observed electrostatic bursts accompanied by chorus should be viewed partly as an instrumentational limitation rather than a definitive region of occurrence.

The frequency of the bursts has always been observed to be below the local plasma frequency (f_p), as determined by the lower edge of the continuum radiation [*Gurnett and Shaw*, 1973]. This difference between the emission frequency and the plasma frequency varies from essentially undetectable, to as much as 60%. The burst frequency was always well above the local electron gyrofrequency as determined by the magnetometer data [*Russell*, 1978]. The bursts always occur in a broad frequency band, as opposed to a sharp monochromatic emission. The bandwidth is usually a few hundred hertz to several kilohertz.

The bursts have been described as electrostatic because no wave magnetic field has been detected in association with them. Typically the broadland electric field strength of the bursts is on the order of 50 μV/m. Because the wave magnetic field remains at the instrument noise level in all cases observed, a limit can be placed on the magnetic to electric field ratio of about $cB/E \lesssim 4$, which corresponds an index of refraction $n \lesssim 4$. Because no electromagnetic plasma wave mode is known to exist with $cB/E \lesssim 4$ in the frequency range $f_g < f_{\text{burst}} < f_p$, the bursts are almost certainly electrostatic. The typical electric and magnetic field strengths of the chorus emissions associated with the electrostatic bursts are about 300 μV/m and 40 pT, respectively.

Serious consideration was given to the possibility that the electrostatic bursts are an instrumental effect. For reasons outlined in *Reinleitner et al.* [1982], which included observations of the electrostatic bursts on IMP 6 data, we have concluded that the bursts are not an instrumental effect. In addition, the good correlation with LEPEDEA electron data shown in section 4 also indicates that the electrostatic bursts accompanying the chorus are not due to an instrumental effect.

The electrostatic bursts have narrowband harmonic structure as shown in *Reinleitner et al.* [1982]. The frequency spacing of the harmonic structure corresponds to the instantaneous emission frequency of the chorus burst. This feature will be discussed again later in this section.

When chorus hooks are found to be correlated with the electrostatic bursts, the onset of the electrostatic burst usually coincides with the minimum frequency of the hook. This relationship suggests that the electrostatic burst may be caused by the increasing phase velocity associated with the rising frequency portion of the hook. It should be noted that the electrostatic burst often continues for a time after the hook has disappeared or merged back into the chorus band.

To identify the mode of propagation of the electrostatic bursts it is useful to try to determine the wavelength and polarization of these waves. The different antenna lengths on ISEE 1 and ISEE 2 have been used to determine the wavelength limits of the bursts. Figure 3 shows an example of the electric field spectrums obtained simultaneously for a long burst that was observed in the wideband data by both ISEE 1 and ISEE 2. These spectrums indicate, when corrected for the antenna length of each spacecraft, that the electric field strengths for both the chorus and the electrostatic bursts are the same at both spacecraft even with different antenna lengths. The fact that the electrostatic burst shows the same electric field strength independent of the antenna length indicates that the wavelength of the burst must also be greater than the length of either antenna [*Gurnett and Frank*, 1978]. Thus the wavelength of the electrostatic bursts must be longer than the ISEE 1 electric dipole antenna, so that $\lambda_{\text{burst}} > 215$ m.

Further studies of the wideband data show that although

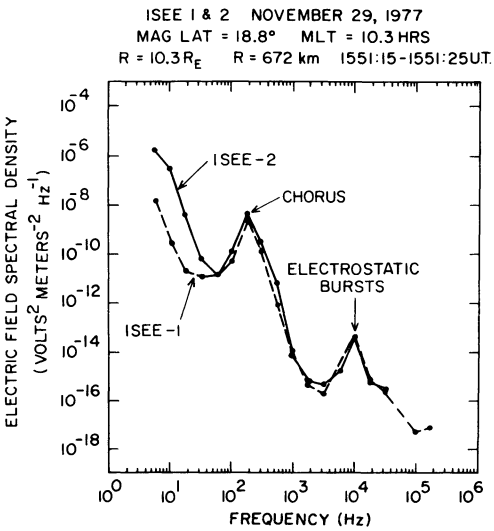

Fig. 3. An example of the electric field spectral density versus frequency taken at both ISEE 1 and ISEE 2 during a long electrostatic burst that was observed at both spacecraft. The electric field spectral density is corrected for the different electric dipole antenna lengths on the two spacecraft. The fact that both the chorus and the electrostatic bursts have almost identical spectral densities indicates that the wavelengths of both waves are significantly longer than either spacecraft antenna.

there is a good correlation between chorus hooks in both ISEE 1 and ISEE 2 data, the detailed correlation between the electrostatic bursts is relatively poor. A strong correlation does exist between the overall occurrence of bursts at the two spacecraft, which is probably due to the correlation between the bursts and the chorus itself. However, a good correlation does not exist between the structure of the individual elements of the bursts. This indicates that the wavelength of the bursts is shorter than the distance between the two spacecraft. Thus we can say that 215 m $\lesssim \lambda_{burst} \lesssim$ 100 km.

The rapid sample data has been used to determine the polarization of the electrostatic bursts. In a case where the channel of the multi-channel electric spectrum analyzer on ISEE 1 was set at about the frequency of the electrostatic burst and was also in the rapid sample mode, it is possible to determine the polarization from the spin modulation of the electric field intensity. An example of this type of polarization analysis is shown in Figure 4, which shows that the electric field of the bursts appears to be aligned with the projection of the ambient magnetic field in the spin plane of the spacecraft. This result indicates that the electrostatic bursts have a wave vector (**k**) generally aligned along the ambient magnetic field. It should be noted here that, even though the long bursts in the wideband data do not show a spin modulation effect because of the AGC, several checks of the spectrum analyzer data show that the spin modulation is present.

Since the wideband data is transmitted from the satellite in analog form and is spectrum analyzed on the ground, it is possible to study the actual waveform as seen by the electric field antenna on the spacecraft. An example is shown in Figure 5. The electric field versus time waveform for both the chorus and electrostatic burst is shown in the lower panel for the very short burst marked in the middle panel at 1739:23 UT. The lower signal is the chorus waveform while the upper high frequency signal is the associated electrostatic burst waveform. Both signals have been processed by bandpass filters to eliminate signals not in the frequency band of interest. As can be seen, the electrostatic noise is actually composed of many shorter bursts of a high-frequency signal that is modulated at the chorus frequency. Thus, the harmonics mentioned earlier are a modulation effect caused by the periodic modulation of the electrostatic noise at the frequency of the chorus emission. In the cases where harmonics are not observed, the electrostatic burst occurs in a broad frequency band that tends to blend any harmonics into a broad continuous spectrum. It is also noted that for the long electrostatic bursts, the modulation effect is either not as strong or nonexistent. This effect is illustrated in Figures 6*a* and 6*b*, which show an example of a good modulation effect on a short burst associated with a hook. In Figures

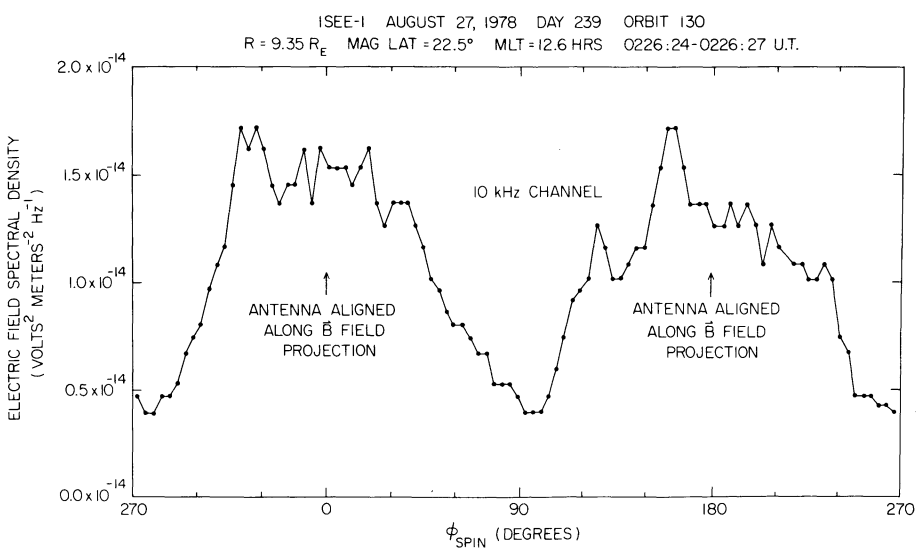

Fig. 4. Rapid sample electric field data for the 10-kHz channel of the multichannel spectrum analyzer showing the longitudinal nature of the electrostatic burst. The burst, centered near 10 kHz, is sampled at 32 samples per second and is plotted against the spin angle ϕ of the spacecraft. As indicated, the maximum electric field strength occurs when the dipole antenna was oriented along the projection of the magnetic field onto the spin plane of the spacecraft. This indicates that the burst is polarized with the electric field aligned along the ambient magnetic field.

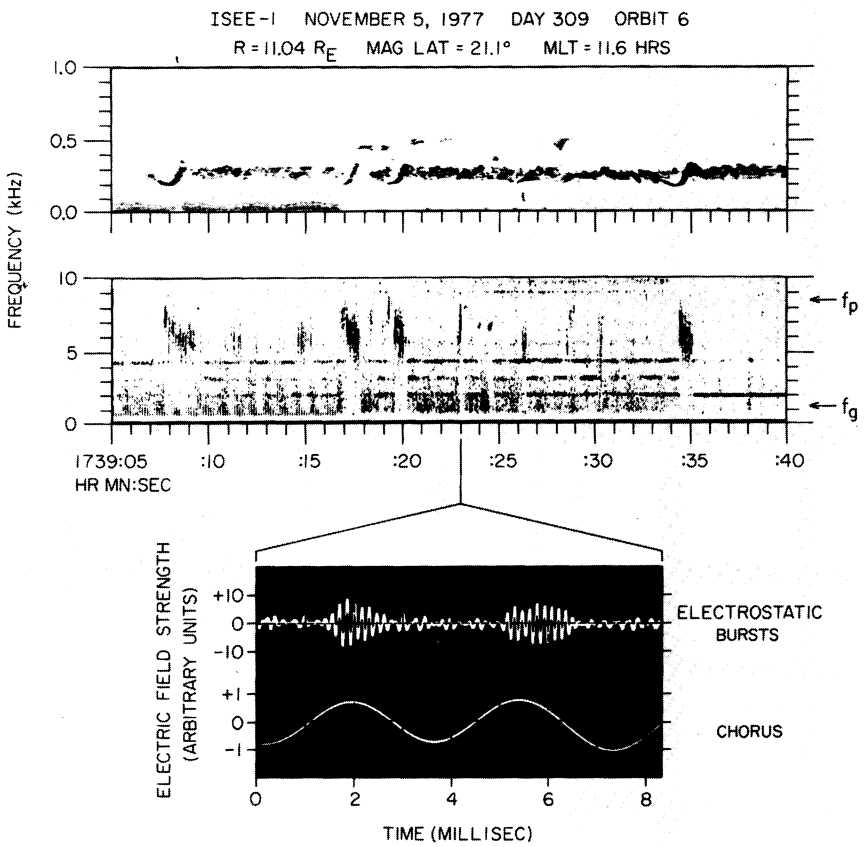

Fig. 5. The lower panel shows the oscilloscope waveform pattern taken from the very short burst indicated in the frequency-time spectrogram. The low-frequency signal in the bottom of the lower panel is the chorus waveform, while the high-frequency signal bursts at the top of the lower panel are the electrostatic bursts. The amplitude of the electrostatic bursts is modulated by the chorus waveform. It should be noted that the duration of the lower panel is only 8 ms.

6*c* and 6*d* a longer burst of about 6 s duration shows a much reduced modulation effect. Owing to possible phase shift effects in the filters used for the waveform analysis and other unknown phase shifts related to the wave normal angle, nothing can be said at this point about the absolute phase relationship between the chorus waveform and the modulation of the electrostatic burst.

To summarize the characteristics covered in this section, we have noted that electrostatic bursts appear to accompany chorus 'hooks' and simple chorus intensifications in the earth's outer magnetosphere. These bursts seem to have a wavelength such that 215 m $\lesssim \lambda_{burst} \lesssim$ 100 km. The electric field vector of the electrostatic bursts is aligned along the ambient magnetic field, and thus the wave vector is also aligned along the magnetic field. Examination of the waveforms for both the chorus and bursts indicate that often the higher frequency waveform for the burst is modulated by the chorus waveform. The strong correlation between the envelope of the electrostatic bursts and the chorus suggests some strong physical interaction between these two wave modes. The fact that the electric field strength of the electrostatic bursts is much less than that of the chorus wave suggests that the bursts are probably caused by the chorus.

3. Model Interpretation of Observational Data

In the previous section, the observations of the electrostatic bursts accompanied by whistler mode chorus were described. This section describes a model that explains the observations. The most obvious characteristic of the bursts is that they are electrostatic and near the electron plasma frequency. This could suggest some form of Langmuir oscillation. However, the fact that the emission frequency occurs below the electron plasma frequency requires some explanation because the Langmuir oscillation always occurs at frequencies near or slightly above the electron plasma frequency. Parametric interactions between the electrostatic mode and the chorus are considered unlikely because the electrostatic bursts sometimes last longer than the chorus burst. Because the wave vector for the bursts is apparently aligned in the general direction of the ambient magnetic field, the observations suggest a two-stream instability with a field-aligned beam.

The general model that is proposed is illustrated in Figure 7. It is well known that whistler mode chorus in the magnetosphere has a wave normal vector that is typically at an oblique angle to the magnetic field [*Burton and Holzer*, 1974]. The top part of Figure 7 shows that when the wave normal angle θ is nonzero, the electric field of the chorus wave has an electric field component $\mathbf{E}_{\|}$ along the $\mathbf{B}_0$ field. Because the ambient magnetic field $\mathbf{B}_0$ in the region of interest is on the order of 40 nT, and the wave magnetic field of the chorus is on the order of 40 pT, it is expected that the first order motion of the electrons will be the usual helical motion along the ambient magnetic field line.

The model, as proposed, assumes that the electrons are free to move along the ambient magnetic field line ($\mathbf{B}_0$), under the influence of the parallel electric field ($\mathbf{E}_{\|}$) of the chorus wave.

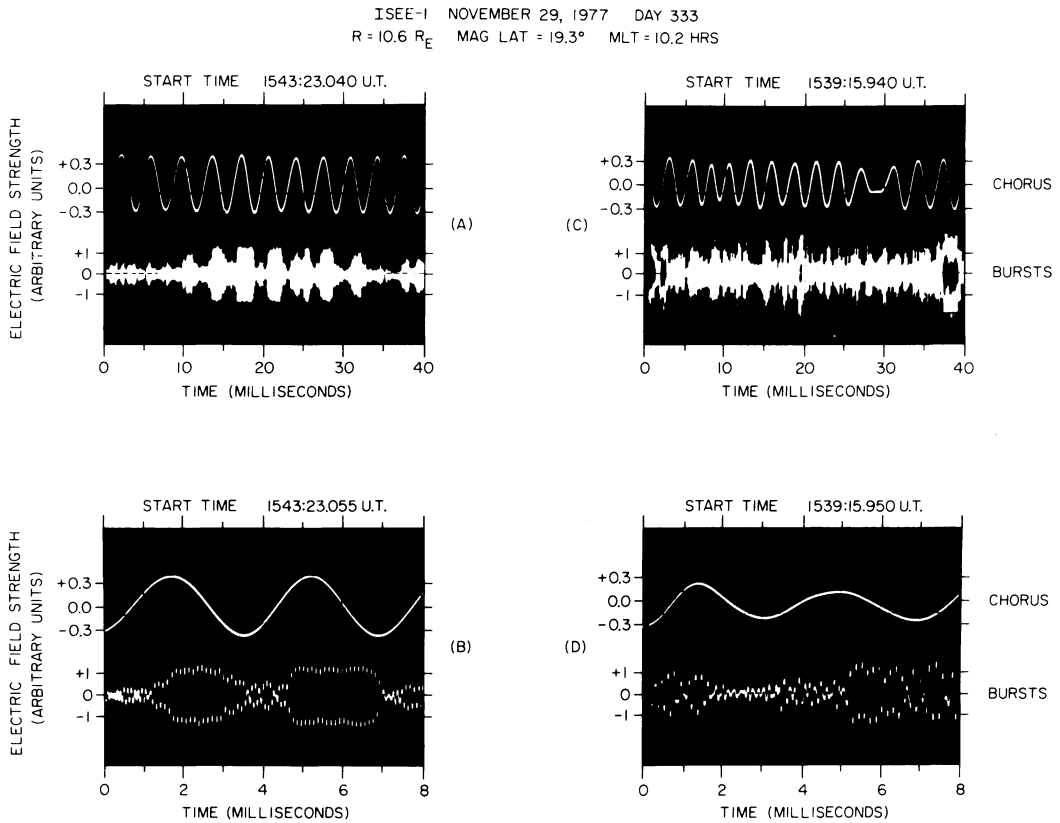

Fig. 6. Four examples of oscilloscope waveform are shown. In all cases the top trace is that of the chorus, while the bottom trace is that of the electrostatic burst. The two left examples (*a* and *b*) are taken from a short burst correlated with a chorus hook (*b*) being an expansion of part of (*a*). The amplitude modulation of the bursts by the chorus waveform is very evident. The two right examples (*c* and *d*) are from a long burst just a few minutes earlier. These again have different time scales, (*d*) being an expansion of (*c*). In this case the amplitude modulation of the electrostatic noise is not closely associated with the chorus waveform.

Thus the electrons will only be affected by an effective potential due to $\mathbf{E}_{\parallel}$ such as that shown in the middle part of Figure 7. This electric field permits electrons to be trapped in effective potential wells of the chorus wave and to be carried along with the chorus wave at the chorus phase velocity.

These trapped electrons will move in bunches at the chorus phase velocity in the effective potential wells and, to a stationary observer, would pass by in a periodic manner with the chorus wave. Because the trapped electrons move at the same velocity, these electrons effectively have a delta function velocity distribution and would therefore be expected to excite electrostatic waves via a two-stream like mechanism. The bursts of electrostatic waves would then be expected to have the modulated characteristics of the short electrostatic bursts as shown in the bottom part of Figure 7.

For the plasma parameters in the region of interest, the index of refraction for the whistler mode is on the order of 10 to 20. This implies a phase velocity of somewhat less than one tenth the velocity of light. From the wavelength and electric field intensity of the chorus wave it is possible to estimate the depth of any possible potential well. A simple calculation (assuming $n = 10$ and $f = 300$ Hz) gives: $\lambda = V_p/f = 100$ km. This wavelength implies that for a chorus wave with an electric field intensity of about 300 μV/m, such as reported in section 2, the potential well would be 100 km $\times$ 300 μV/m = 30 V. This value is encouraging, as it is large enough to be a significant potential well for electrons with energies of a few keV. With an index of refraction of about 10 or 20, the electrons moving at the chorus phase velocity will have an energy of ≈ 2 keV or less.

Early work on resonances by *Kennel and Petchek* [1966] concentrated on studies of electron cyclotron resonance interactions ($m = 1, 2, \ldots$ in (1)). The possibility of particle trapping by Landau resonance interactions ($m = 0$ in (1)) with chorus waves has only recently been considered. *Nunn* [1971, 1973] investigated the trapping of particles by Landau resonant interactions with electrostatic waves. A more recent work by *Inan and Tkalcevic* [1982] deals with the nonlinear equations of motion for particles in Landau resonance with chorus waves. The work of *Inan and Tkalcevic* [1982] is greatly extended in a doctoral dissertation by S. Tkalcevic [1982] in which the Landau resonant trapping properties of whistler mode waves are explored. His computer model simulations yield several important new results and conclusions, including the finding that an intensity threshold exists, below which trapping is not possible. This threshold depends on several parameters, most notably the wave vector angle θ from the $\mathbf{B}_0$ field, and is in general on the order of $E_{0\parallel} \approx 20$ μV/m. In all cases of the observation of electrostatic bursts, the chorus intensity was well above this threshold, usually on the order of $E_0 \approx 300$ μV/m.

To demonstrate the trapping of electrons at the Landau resonance for the specific parameters relevant to this study, a computer simulation was performed by solving for the motion of an electron in the presence of a whistler mode wave propagating at an angle to the $\mathbf{B}_0$ field. Using the cold plasma

dispersion relation given by *Stix* [1962], equations for the electric and magnetic field components of a whistler mode wave can be obtained [*Reinleitner*, 1982]. The computer model uses a box with the z axis along the **k** vector of the wave and a length of one wavelength. This model gives periodic boundary conditions on the box where the x and y lengths are arbitrary. The electric and magnetic fields in the box are thus only functions of the z axis position and time. The electron is injected at a velocity slightly greater than the wave phase velocity projected along the ambient magnetic field, and the wave intensity is allowed to grow linearly with time. The fourth order Runge-Kutta method is used to solve the first order equations for the acceleration and position as a function of time. The time step is about one-twentieth of the electron cyclotron period.

The results for three different wave vector angles θ are shown in Figure 8. The parameters used are $\omega = 1885\ s^{-1}$, $n_e = 1.0\ cm^{-3}$ and $B_0 = 40$ nT, which are typical for the events illustrated in Figures 1 and 2. Trapping occurs when the whistler mode intensity exceeds a threshold intensity. In this illustration $V_p/\cos\theta$ is the projected wave phase velocity along the ambient magnetic field ($\mathbf{B}_0$), V_z is the initial particle velocity along $\mathbf{B}_0$, and ΔE is the energy difference between an electron moving at $V_p/\cos\theta$ and one moving at V_z. Z phase is the relative phase between the electron position and the wave front. Trapping is defined as the point in time when the phase variation of z phase becomes bounded. Trapping occurs when the electric field amplitude E_0 becomes large enough to produce bounded oscillatory motion (on the order of 40—80 μV/m). The results obtained show that the required E_0 for trapping decreases as the wave vector angle θ increases. These computer simulations show that particle trapping occurs at electric field intensities that are consistent with those found in *Tkalcevic* [1982].

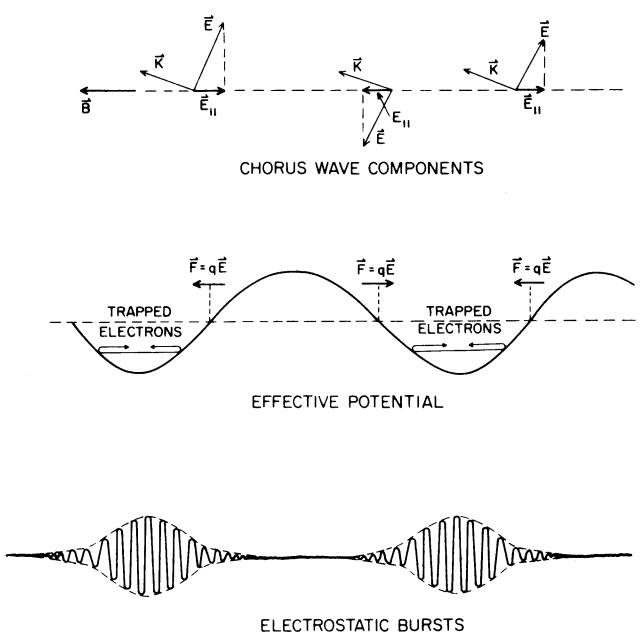

Fig. 7. Illustration of the model proposed for whistler mode electron trapping and burst generation. The top panel shows how a wave propagating at an angle to $\mathbf{B}_0$ produces an $\mathbf{E}_{\|}$ (parallel) field, while the middle panel illustrates how an electron moving along the magnetic field line sees an effective potential associated with $\mathbf{E}_{\|}$ and can be trapped at the whistler mode phase velocity. The lower panel shows how these trapped electrons can generate electrostatic emissions modulated at the chorus phase velocity.

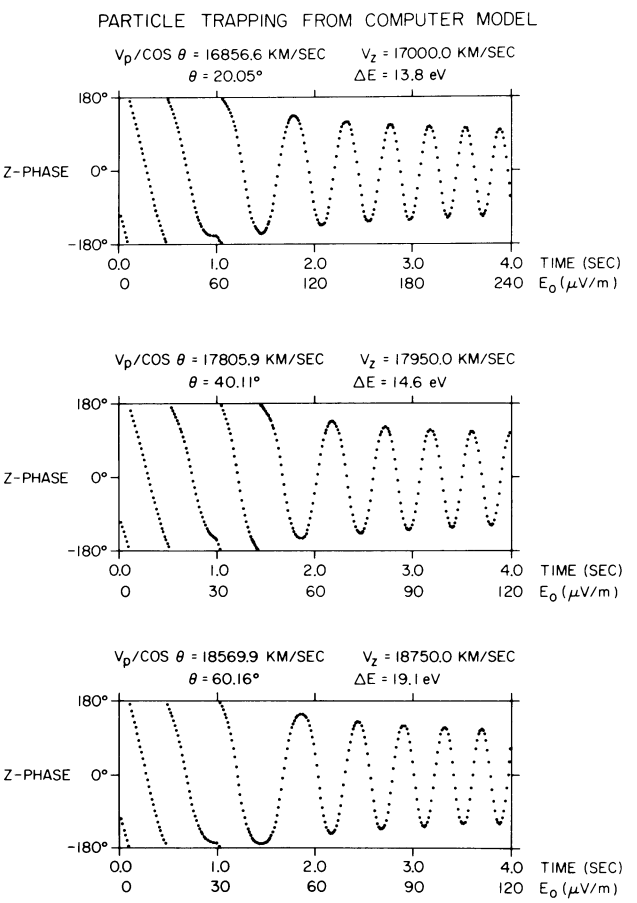

Fig. 8. Three cases of particle trapping produced by computer modeling for different wave vector angles (θ) to the ambient magnetic field. Z phase is the phase relation between the electron and the whistler mode wave. Trapping occurs when the phase variation is bounded. In the model, the electric field intensity of the whistler mode wave increases linearly with time, and so the abscissa is marked as both time and E_0.

Electrons may be trapped in the potential well of the chorus wave by an increase in the component of the wave electric field aligned along the ambient magnetic field, as was illustrated in the described particle simulation. This increase is expected from either of two possible mechanisms. First, the electric field may increase as the chorus grows in amplitude near the equatorial plane. Second, the wave vector angle θ may increase as the chorus propagates away from the equator as suggested by *Thorne and Kennel* [1967], thereby increasing the parallel component of the wave electric field. Both methods could, of course, be occurring simultaneously.

Electrons may also be detrapped by several possible mechanisms. Mutual electrostatic repulsion due to too many trapped electrons could push some of the electrons out of the potential well (Poisson's equation is neglected for the simulation). The chorus wave may accelerate in phase velocity at a rate sufficiently great to dump electrons out of the potential wells. This mechanism could prove a very effective method of detrapping the electrons if any slight but sudden density irregularities are encountered along the field line. Also, as the wave propagates into regions of stronger magnetic field, the magnetic moment force, $-\mu\partial B/\partial z$, can become large enough to detrap the electrons.

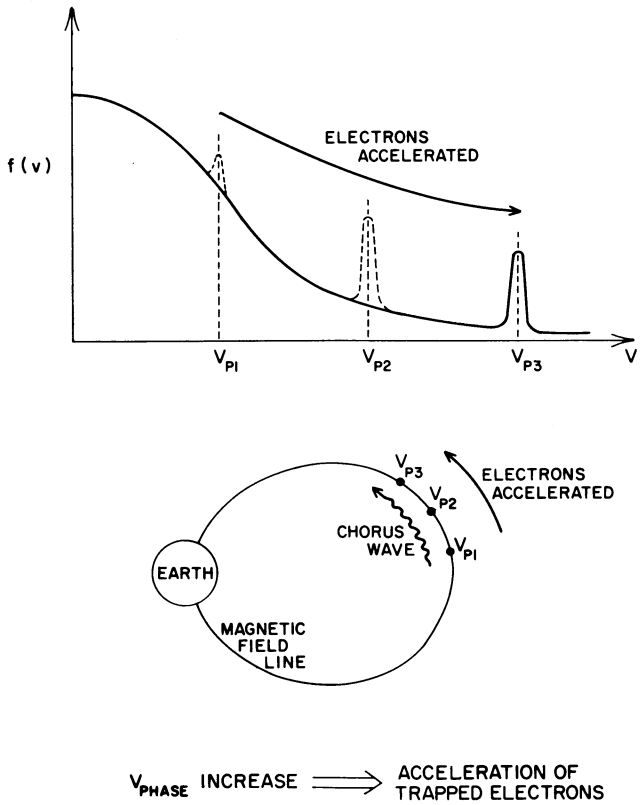

Fig. 9. Illustration of a possible mechanism for producing a distinct electron beam in the electron distribution function. In this suggested scenerio, the chorus phase velocity increases and the trapped electrons are accelerated to higher velocities. The velocity increase has been exaggerated for clarity.

Trapping alone would probably not explain enough electron enhancement at the chorus phase velocity to create a two-stream bump on tail instability, since trapped electrons oscillating in the potential well still have the same range of velocity as before trapping occurs. Some mechanism is required to translate these electrons into a region of velocity space with a lower phase space density so that a double-humped velocity distribution is produced. A likely candidate is some form of acceleration or deceleration in which the chorus first traps the electrons as the wave grows in amplitude and then changes the velocity of the trapped electrons. This process is illustrated in Figure 9, where a chorus wave generated at the equator propagates along the magnetic field line to higher latitudes. As the wave packet moves to higher latitudes, the magnetic field strength increases, thereby increasing the phase velocity and accelerating any electrons that were trapped by the wave. The increase in the magnetic field strength is, of course, in competition with the increasing plasma density at higher latitudes that would tend to increase the index of refraction. Because of the high electron temperature in the region, it is not clear which trend would dominate. Another possible acceleration mechanism is suggested by the hooks, such as those in Figure 5. The electrostatic burst usually seems to be associated with the rising portion of the hook. As the frequency of the hook rises, the index of refraction decreases, thereby increasing the phase velocity. This frequency variation can accelerate electrons trapped in the wave packet to higher velocities. It should be emphasized that large velocity changes are not required. Relatively small velocity changes can 'pile up' electrons and create a positive slope in the distribution function, thereby causing the electrostatic instability.

The exact method by which the chorus phase velocity changes to create a positive slope in the distribution function has not been clearly established. Some change in the chorus phase velocity is, however, required. The effect of the changing phase velocity is to move part of the distribution function to higher or lower velocities, thereby creating a bump in the new distribution function as illustrated in Figure 9. Only a small change in the phase velocity would be necessary for a two-stream instability to arise if the trapped electrons have a sufficiently narrow velocity spread.

4. Electron Distribution Functions

The most obvious feature predicted by the model described in section 3 is the existence of the enhanced trapped electrons that should be moving at the phase velocity of the chorus wave. Knowing the plasma frequency from the cutoff of the continuum radiation, the 64 s averaged magnetic field from the data pool tape, and the chorus frequency as obtained from the wideband data, it is possible to determine the phase velocity of the whistler mode wave. The only unknown parameter is the wave normal angle θ. The phase velocity is, however, only weakly dependent upon θ, unless θ is quite large. Using the theoretical value of the phase velocity, a search for an electron beam aligned along the $\mathbf{B}_0$ field was performed by using the LEPEDEA instrument on ISEE 1.

Several difficulties arise in using particle data to search for this electron beam. The main limitation in the LEPEDEA instrument for this purpose is the time required for a full energy scan. An entire three-dimensional distribution function requires about 2 min (128 s) when the satellite is in the high bit rate mode, while most electrostatic bursts are much shorter than a 2-min duration. Short bursts accompanying chorus hooks are not likely to be observed with the LEPEDEA data. A careful study was made of the ISEE 1 wideband data to find cases where the electrostatic burst was long enough for an effective study of the LEPEDEA data. Ten possibilities were found where either one long electrostatic burst or several shorter electrostatic bursts covered at least 70% of a 2-min period in the wideband data. These possibilities were checked with detailed computer listings of the LEPEDEA instrument responses. We anticipated that a beam would not be detected in some of these cases due to several factors. Since only a few energy scans from the full 128-s energy cycle will be at the correct energy to detect the beam, there is a high probability that the burst would not be occurring at the appropriate sample time. In addition, the plasma density in the outer magnetosphere is usually very low, typically less than 1 electron cm^{-3}, so that plasma analyzers often obtain relatively low responses in this region. Out of the ten selected cases, three showed no clear sign of any beamlike enhancement, and seven showed some detection of an electron enhancement. This enhancement is referred to as a beam in this paper, though careful examination shows that it does not correspond to an idealized delta function beam. Owing to limitations of computer time, only the two best cases in the instrument response listings were analyzed in detail.

In the E-ϕ spectrogram of Figure 10, detectors 2E and 6E are the detectors that point along the ambient magnetic field line as determined from the orientation of the spacecraft and the magnetic field data from the magnetometer experiment [*Russell*, 1978]. The horizontal axis in each spectrogram is the rotational angle ϕ of the spacecraft and the vertical axis is the particle

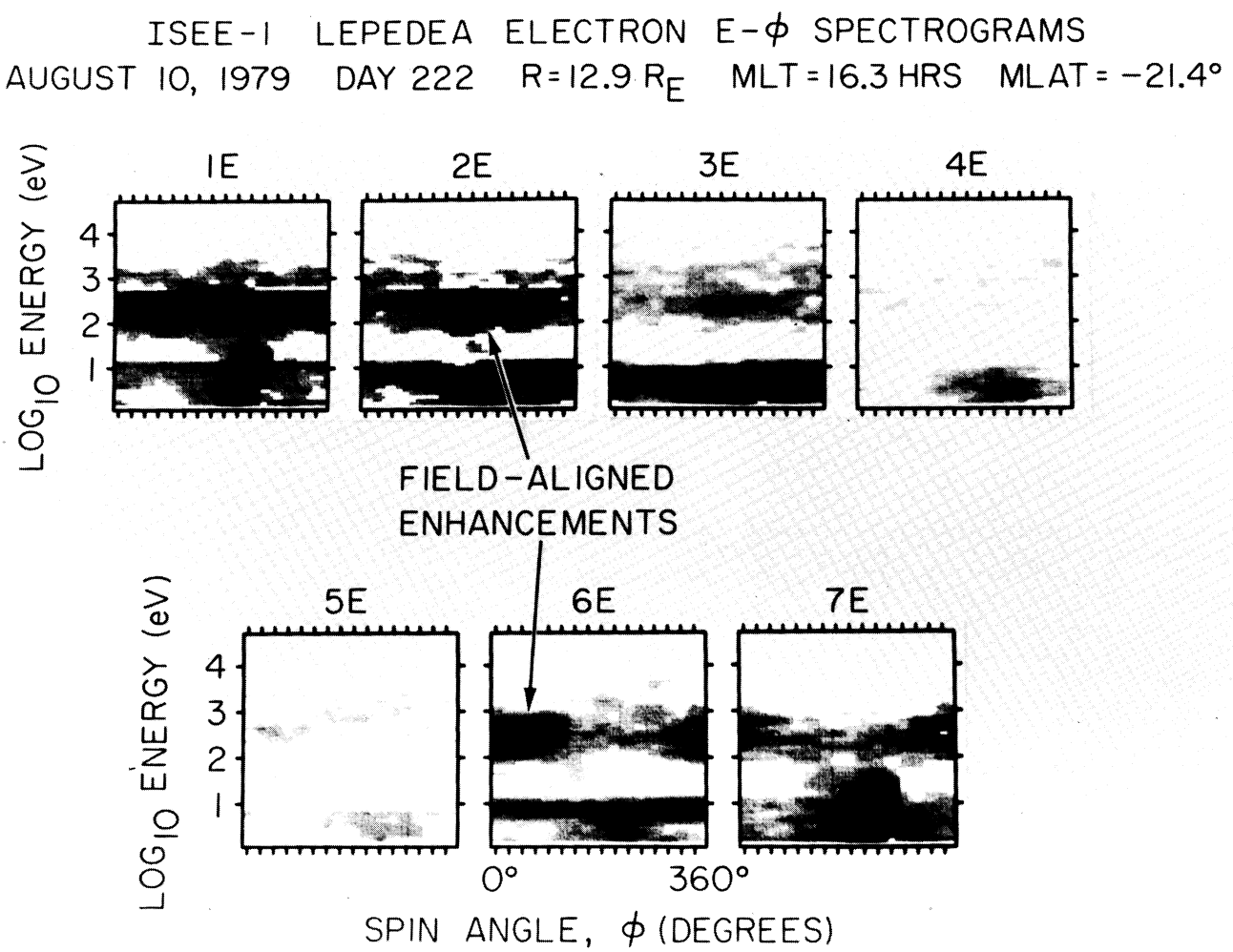

Fig. 10. E-ϕ spectrogram of electrons for day 222 of 1979 from the LEPEDEA data. The beamlike features indicated by the arrows are the magnetic field-aligned electron enhancements, which occur simultaneously with the long electrostatic burst. Only detectors 2E and 6E point in the $\pm\mathbf{B}_0$ directions at opposite spin angles (ϕ) for this event.

energy (P for protons and E for electrons). The magnetometer data shows that features labeled 'field-aligned enhancements' occur when the detector is pointing along the magnetic field. Thus, the enhancements are field-aligned, which is the expected direction for a beam in Landau resonance with the chorus.

One clear feature that emerges from Figure 10 is that there are actually two counterstreaming electron enhancements at the same energy. This effect is easily understood if the bounce time for a mirroring particle is examined. From *Van Allen* [1962], an equation for the bounce time of an electron trapped in the earth's geomagnetic field is given by

$$\tau_2 = 0.85(r_0/\beta)\ T(\alpha_0)\ \text{s} \qquad (2)$$

In this equation r_0 is the equatorial radial distance in earth radii, β is v/c, and $T(\alpha_0)$ is a parameter ranging from about 0.56 to 1.3. Thus the bounce period for $r_0 \approx 10\ R_E$, $\beta \approx 1/10$, and $T(\alpha_0) \approx 1$ is $\tau_2 = 8.5$ s. This estimate shows that the bounce period is on the order of 10 seconds. Thus for long bursts, such as the ones examined in this study, the electrons will be mirroring back and forth along the field line and will show up in the LEPEDEA data as a symmetric field-aligned distribution.

It is also worth noting here that the LEPEDEA instrument is not expected to temporally resolve the modulated or periodic nature of the electron enhancements. The instrument averages over a 0.25-s sample interval. It is expected that for the long bursts, the spatial bunching of the electrons is no longer occurring. In the waveform studies of the long bursts, the modulation effect is not very dominant and is often completely absent. A very strong possibility exists that any electron trapping and acceleration may be occurring at some other location along the field line, and that the electron enhancements observed by the LEPEDEA instrument are no longer moving at the local chorus phase velocity.

For the case in Figure 10, on day 222/79, the following plasma characteristics were noted: $f_p \approx 5.7$ kHz, $f_{\text{chorus}} \approx 150$ Hz, and $\mathbf{B}_0 = 25.1$ nT. These parameters yielded a value for the index of refraction of 19.8, which would correspond to electrons moving with an energy of 650 eV ($\pm 40\%$), while the center of the enhancement in Figure 10 is at 630 eV ($\pm 20\%$). This close agreement should be regarded as somewhat fortuitious, since for the second case on day 263/80, the agreement is less exact. The plasma parameters for the second case are $f_p \approx 6.5$ kHz, $f_{\text{chorus}} \approx 400$ Hz, and $\mathbf{B}_0 = 30.8$ nT. These parameters yield a value for the index of refraction of 15.1, which would correspond to an electron moving with an energy of 1120 eV ($\pm 30\%$), while the center of the enhancement was at 400 eV ($\pm 20\%$). Because the local chorus phase velocity and the beam velocity differ by a significant amount ($V \propto$

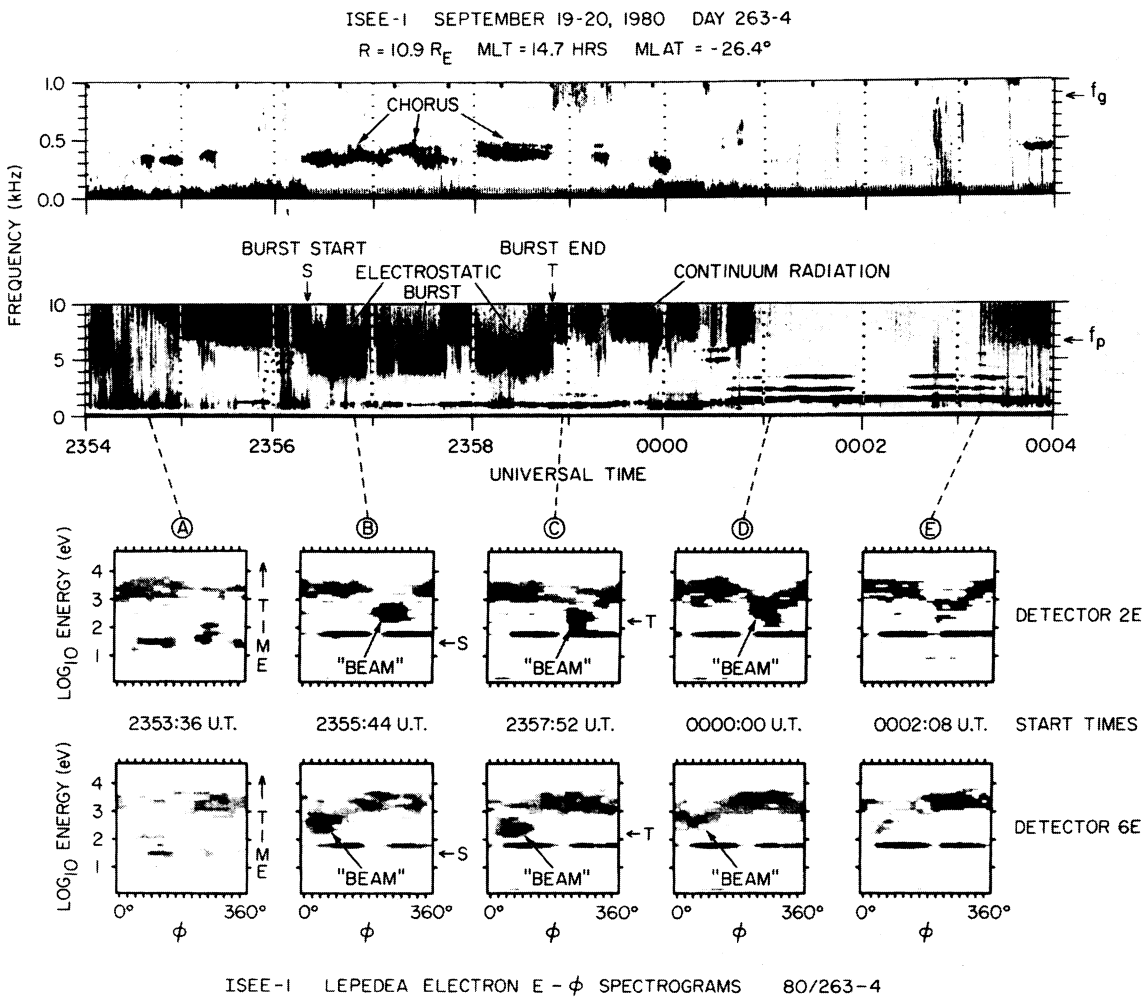

Fig. 11. A composite figure showing the correspondence between a very long electrostatic burst and the field-aligned electron beams shown in the LEPEDEA data. The upper panels are frequency-time wideband data from ISEE 1 showing a 2.5-min burst with the start time marked with an S and the end time marked with a T. The lower panels are a time mosaic of detectors 2E and 6E from the E-ϕ spectrograms for approximately the same 10-min interval. Both time and energy increase along the ordinate of each E-ϕ spectrogram. The ϕ-independent enhancements below the beam energy at about 100 eV are associated with photoelectrons. It is clear that the field-aligned enhancement at $\approx$ 400 eV is strongest during the burst period, although it also persists at lower intensities for several minutes after the termination of the burst.

$\sqrt{\text{Energy}}$), the acceleration of the $\approx$400 eV electrons is probably taking place somewhere else along the magnetic field line. In this case, the beam electrons may have been accelerated by a change in the chorus phase velocity before escaping from the potential well through one of the mechanisms described in section 3.

In both of the cases examined the electron enhancements were found to occur in the E-ϕ spectrograms when the long duration burst appeared, and to persist for several minutes afterward, fading out gradually, rather than abruptly turning off as the electrostatic burst does. The case of day 263/80 is shown in Figure 11. The upper portion of Figure 11 shows a standard case of wideband data from ISEE 1 for September 19–20, 1980. In this figure the chorus shows up clearly as a dark band in the upper panel at about 300 Hz. The electrostatic burst shows up as a dark band in the lower panel from about 3.5–7.0 kHz. The fact that the continuum radiation from about 6.5–10 kHz ceases when the electrostatic burst appears is caused by the AGC, because the burst is of much greater intensity than the continuum radiation. The time scale is much longer than other wideband figures in this work. It covers a period of 10 min with the 2.5 min electrostatic burst labeled at its start time with an S, and its end time with a T. There is a long period after the end of the burst with little or no chorus and burst activity.

The lower portion of Figure 11 shows a time series of E-ϕ spectrogram panels for the same time period. Only detectors 2E and 6E are important in this time period as they show the field-aligned electron beams very clearly. These beams are also aligned along the ambient magnetic field. Time as well as energy is given on the ordinate of each detector panel with a time of $\approx$128 s per panel. The start times of each panel are given between the corresponding detector panels. The start time of the burst is indicated by S, and the end time by a T. As can be seen, the field-aligned electron enhancement is strongest during the burst, and gradually fades away. A clear relationship is evident in this data between the simultaneously occurring chorus and burst, and the field-aligned electron enhancements or 'beams.' The gradual fading out of the beams after the end of the electrostatic bursts may be accounted for by the mirroring electrons bouncing back and forth between their conjugate mirror points several times before being lost.

A perspective plot showing the entire electron distribution function for a 2-min interval on day 222 in 1979 is shown in Figure 12. This plot corresponds to the event shown in Figure 10. The perspective plot clearly shows the field-aligned enhancements. By integrating over just the enhancement and subtracting the distribution without the enhancement, a value for the beam density can be obtained. The value of the beam density divided by the plasma density is 2.5×10^{-3} for the positive $v_{\|}$ enhancement, and 1.3×10^{-3} for the negative $v_{\|}$ enhancement. If a cold electron component exists that is not detected by the LEPEDEA instrument, then these values would have to be lowered slightly. From the plasma density values estimated from the continuum radiation cutoff in the wideband data, these values would have to be lowered by about a factor of ≈ 2. The field-aligned electron enhancements are therefore about three orders of magnitude less than the ambient plasma density.

If an energy gain of about 30 eV is postulated for each electron in the enhancement, and the chorus wave is assumed to have a magnetic field intensity of approximately 40 pT, the wave energy density of the chorus is approximately the same as the energy gain per unit volume for the electron enhancement. An example of this process might be electrons in the distribution function increasing from 600 eV to 630 eV, producing an enhancement at 630 eV in the distribution. Most of the chorus wave energy resides in the wave magnetic field. The chorus wave energy appears to be adequate to create the electron beam. The electric field energy density of the electrostatic burst is about three orders of magnitude less than the energy density of the chorus wave if the value of 50 μV/m is used. Thus, energy considerations for the model outlined in section 3 would appear to be satisfied.

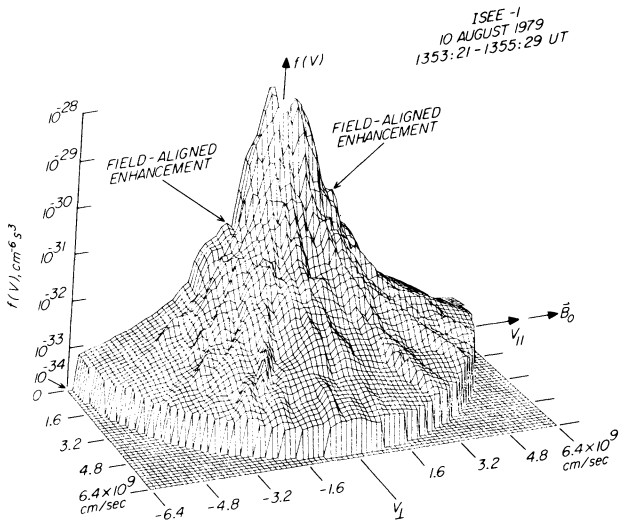

Fig. 12. Perspective plot of the electron distribution function from the LEPEDEA data for day 222 of 1979. The two field-aligned electron enhancements are indicated.

5. The Theory of the Resistive Medium Instability and Its Comparison to Observations

The standard two-stream theory, as described in most introductory plasma physics texts such as *Krall and Trivelpiece* [1973], is not adequate to describe the observations of the electrostatic bursts. The primary difficulty is that for a simple bump on tail distribution function the frequency of maximum growth rate is predicted to be near or slightly above the electron plasma frequency, $\omega^2 = \omega_{pe}^2 + 3\langle v_z^2 \rangle k^2$, whereas the bursts usually occur below the electron plasma frequency.

This difficulty is partially resolved if a finite beam density is considered, as in equations 1.51 and 1.52 from *Mikhailovskii* [1974]. Mikhailovskii's derivation assumes a finite and small beam density represented by the parameter $\alpha \ll 1$ where $\alpha = n_b/n_e$, n_b is the beam density, and n_e is the plasma electron density. Using a simple Taylor expansion about ω_{pe}, the first order corrections to the dispersion relation can be obtained with the result that the frequency and growth rate are given by

$$Re\ \omega = \omega_{pe}\left[1 - \frac{\alpha^{1/3}}{(2)^{4/3}}\right] \tag{3}$$

and

$$Im\ \omega = \omega_{pe}\frac{\sqrt{3}}{(2)^{4/3}}\alpha^{1/3} \tag{4}$$

This finite beam approximation provides a reasonable growth rate for the instability, and a reduction in the frequency of the oscillation below the plasma frequency. The reduction in the frequency below the plasma frequency is, however, not sufficient to explain the large (60%) reductions sometimes observed for the electrostatic bursts unless a totally unreasonable beam density is assumed ($\alpha \simeq 1$). Such a large beam density would likewise invalidate the assumption that $\alpha \ll 1$. In section 4, we found that the LEPEDEA data yielded $\alpha \approx 10^{-3}$.

A different type of instability that explains many of the above difficulties is discussed in *Briggs* [1964]. This instability is called the resistive medium instability. The derivation of this instability is outlined in appendix A. This derivation is made for a one-dimensional system. It assumes a weak beam system with the beam and the background plasma ions being cold but with the background electrons being warm. In this derivation, a resonance distribution was used for the background electrons for mathematical simplicity. The derivation in fact shows two types of instabilities, called the reactive medium instability and the resistive medium instability, both of which are important under different regimes of V_0/V_T, where V_0 is the 'beam' velocity and V_T is the rms thermal velocity.

The reactive-medium instability has a large growth rate when $V_0 \gg V_T$ and is essentially the normal bump on tail two-stream instability, yielding results virtually identical to equations (3) and (4). The resistive medium instability is a different type of instability that requires dissipation and occurs when V_0 is on the order of V_T. This condition means that Landau damping is essential to the instability and that the beam must be on the slope of the distribution, not on the tail. The resistive medium instability only occurs for very low velocity beams or plasmas with very hot electrons. This latter case applies to the outer magnetosphere. The thermal velocity in the regions of interest corresponds to electron energies in the range of 200–600 eV. Thus for electron beams with energies from 200 eV to 2 keV, we are well in the range of the resistive-medium instability.

With the use of (7), (8), and (9) derived in appendix A, a plot can be made of the imaginary component of ω versus the real part of ω. The entire imaginary component of ω is contained in $\delta\omega$ and, from equation (A7), it is seen that the imaginary part is always multiplied by ω_{pb}, the plasma frequency due to the beam alone. Thus the growth rate is directly related to the beam density. Figure 13 shows the growth rate as a function of the frequency where ω_i is scaled by ω_{pb}, and the real frequency is scaled by ω_{pe}. Several cases of V_0/V_T are shown. From this

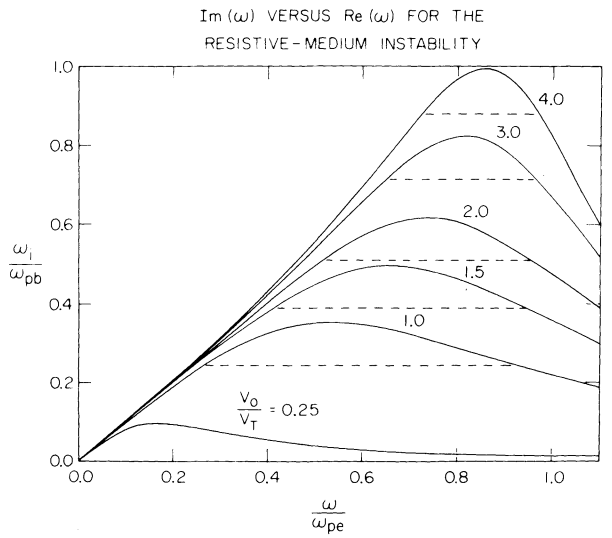

Fig. 13. Graph of the imaginary component of ω versus the real component of ω for the resistive medium instability with several different values of V_0/V_T. The downshift in the frequency of maximum growth rate below the plasma frequency (ω_{pe}) for progressively lower values of V_0/V_T is clearly evident. The dotted lines are used to calculate the points labeled 'theory' in Figure 15.

illustration it is very clearly seen that for cases where V_0/V_T is close to 1, there is a very significant downshift in the frequency of maximum growth rate below the electron plasma frequency. This downshift below ω_{pe} is easier to understand from Figure 14 in which the frequency of maximum growth is plotted versus V_0/V_T. Since the electron beams actually observed have energies of 400 eV and 630 eV, and the thermal velocity in the outer magnetosphere corresponds to electron energies in the range of $\approx$ 200–600 eV, it is seen from this figure that the downshift in frequency below the plasma frequency can vary from a few percent to 60%, in agreement with observations.

The absolute growth rates predicted by the theory must match the growth rates shown in Figures 5 and 6 for the burst waveforms. If $\omega_i = 1/\tau$, where τ is the time required for the envelope of a modulated burst to increase by a factor of e, then

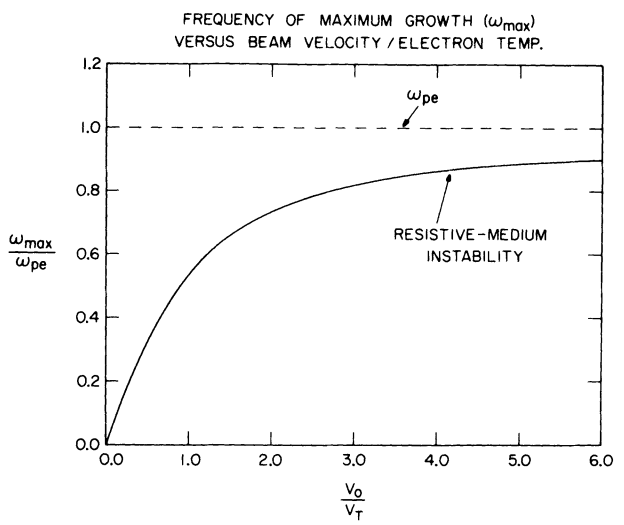

Fig. 14. Graph of the frequency of the maximum growth rate of the resistive medium instability versus V_0/V_T. This plot shows that the frequency of maximum growth rate is shifted well below the plasma frequency for small values for V_0/V_T.

to an order of magnitude from the theory as graphed in Figure 13, $\omega_i/\omega_{pb} \simeq 1$. From the waveforms in Figures 5 and 6 we also observe that $\omega_i/\omega_{pe} \simeq 3 \times 10^{-2}$. These experimental values lead to the conclusion that $\omega_{pb}/\omega_{pe} \simeq 3 \times 10^{-2}$, which implies that

$$\alpha = \frac{n_b}{n_e} \approx \left(\frac{\omega_{pb}}{\omega_{pe}}\right)^2 \simeq 10^{-3}$$

This value, predicted from the theory and the experimentally determined growth rate, indicates that the beam density should be about three orders of magnitude less than the plasma density, which is in agreement with the LEPEDEA results. Thus, the absolute growth rate predicted by the theory is of the correct magnitude as compared to the observed growth rates and the LEPEDEA beam density results.

Another important factor is noted in the curves of Figure 13. As V_0/V_T increases, the peak in the growth curves becomes narrower. This dependence predicts a tendency that had not initially been noticed in the wideband data, namely that electrostatic bursts that are downshifted in frequency by a large percentage of f_p tend to have a wider spread in the frequency. This tendency is illustrated in Figure 15, which shows the spread in the observed frequencies divided by the center of the burst versus the center of the burst frequency divided by the plasma frequency. Figure 15 indicates that a clear correlation exists between these two observed characteristics of the electrostatic bursts.

In order to obtain some idea what the theoretical relationship between these two parameters should be, an examination was made of the range of growth rates expected to be observed in the wideband data. The range in intensity observable in the wideband data is better than 10 dB. If one assumes that the amplitude of the burst at a particular frequency is dependent on the imaginary component of ω at that frequency, then the spread of frequencies observed in the wideband spectrograms will be those frequencies that have an amplitude within 10 dB of the central frequency of maximum amplitude. Estimates show that the ratio of the reduction in the growth rate ω_i that is visible in the wideband data, to that growth rate ω_i that is just barely detectable in the wideband data, is a constant factor [*Reinleitner*, 1982]. Taking a case from Figure 13 where

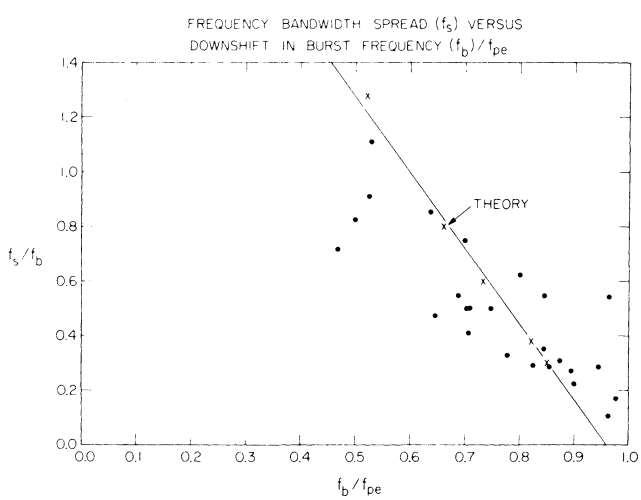

Fig. 15. Plot of observed points in the wideband data showing the frequency bandwidth spread versus the downshift in the burst frequency below the plasma frequency. The theoretical points were computed by using the graph shown in Figure 13.

$\omega/\omega_{pe} = 0.85$, we observe from Figure 15 that the corresponding frequency spread is $f_s/f_b \approx 0.3$. In Figure 13 a dotted line indicating $f_s/f_b \approx 0.3$ (where f_s is the frequency spread of the burst and f_b is the center frequency of the burst) is drawn on the ω_i curve for $V_0/V_T = 4.0$. Using the same ω_i reduction for the other curves gives the solid line in Figure 15. This comparison shows that the observed frequency spread matches the theory extremely well.

The model predicts that the electrostatic bursts should have a phase velocity of approximately the beam velocity. If the phase velocity is 1/20 the speed of light (corresponding to a 640-eV electron beam), and the burst frequency is 10 kHz, then $\lambda_{burst} = 1.5$ km. This wavelength is in agreement with the observationally determined limits on λ_{burst} given in section 2. The resistive medium instability has thus been shown to be in agreement with essentially all of the characteristics of the electrostatic bursts.

This study could also prove useful in understanding certain phenomenon in regions other than the earth's outer magnetosphere. Phenomena similar to the electrostatic bursts described in this paper have been observed in the Voyager 1 wideband data. The Voyager data were taken in the outer Saturnian magnetosphere, on the dayside of Saturn, very similar to the situation in the earth's magnetosphere.

A report by *Kennel et al.* [1980] using data from the ISEE 3 spacecraft described correlated whistler mode and electron plasma oscillation bursts in the solar wind with characteristics very similar to the waves described in this report. This spacecraft is in a halo orbit around the earth-sun line about 235 R_E upstream from the earth. Because the ISEE 3 spacecraft lacked wideband instrumentation, it was not possible to obtain waveform measurements comparable to those obtained from ISEE 1. It is thus not clear whether the 'electron plasma oscillations' reported by *Kennel et al.* [1980] were being modulated by the chorus wave in the same way as in the ISEE 1 data. However, we now regard the Landau resonance interaction described in this paper to be a better explanation for the ISEE 3 observations than the secondary impulsive electron heating mechanism proposed by *Kennel et al.* [1980].

Another possible application of this work is to the study of electron microbursts in the auroral zone [*Oliven and Gurnett*, 1968]. The energetic electron precipitation (> 10 keV) causing these microbursts is usually attributed to pitch angle scattering associated with the generation of chorus. However, at high magnetic latitudes trapping and acceleration of electrons by Landau resonant interactions with whistler mode chorus could produce these electrons.

Thus, the interaction between the whistler mode chorus waves and the observed electrostatic bursts described in this study would appear to have possible relevence in a large number of space physics phenomena. Though this interaction is best understood for the earth's outer magnetosphere, it could explain some features in other space physics data that are not presently understood.

6. Conclusions

This study has revealed several new aspects of wave particle interactions in the earth's outer magnetosphere. It has described the observational characteristics of a type of electrostatic burst that is strongly associated with whistler mode chorus waves. A simple model was developed that explains these electrostatic bursts by the trapping and acceleration of electrons in Landau resonance with the electromagnetic chorus wave. This simple model is supported by a computer particle simulation of an electron interacting with a growing chorus wave that indicates that trapping should occur. By any of several mechanisms the chorus wave phase velocity could increase, accelerating any electrons trapped in Landau resonance with the chorus wave. This acceleration is in many respects similar to the traveling wave linear particle accelerators used in high energy physics. Results from the LEPEDEA data show a significant field-aligned electron enhancement or beam at approximately the chorus phase velocity when chorus waves and electrostatic bursts of long duration are observed.

We conclude that the resistive medium instability can account for the generation of the electrostatic bursts by trapped electrons. This instability is valid where the beam velocity is on the order of the plasma electron thermal velocity, which is shown to be the case for the region of interest based on simultaneous plasma data. The resistive medium instability provides an explanation of the downshift in frequency of the bursts below the local plasma frequency. In addition, the theory predicts a relationship between the frequency spread of the bursts and the frequency downshift for the burst that is in good agreement with the observed spectrum. Overall, very strong evidence is presented that Landau interactions with whistler mode chorus is occurring and that the resistive medium instability is the mechanism responsible for the generation of the associated electrostatic bursts.

Appendix A: Derivation of Resistive Medium Instability Equations

This derivation is very similar to that derived in *Briggs* [1964]. The derivation is made for a one-dimensional system and utilizes a dispersion relation for a weak electron beam ($n_b \ll n_e$) streaming through a plasma, where both the electron beam and the plasma ions are cold. The background plasma electrons are warm. The dispersion relation for such a system is given in *Briggs* [1964] as

$$\frac{\omega_{pb}^2}{(\omega - kV_0)} = K_{||}(\omega, k) \tag{A1}$$

where

$$K_{||}(\omega, k) = 1 - \frac{\omega_{pi}^2}{\omega^2} - \omega_{pe}^2 \int \frac{f_{0e}(v_z)dv_z}{(\omega - kv_z)^2} \tag{A2}$$

is the longitudinal dielectric constant of the plasma in the absence of the beam, V_0 is the beam velocity, ω_{pe} and ω_{pi} are the electron and ion plasma frequencies, ω_{pb} is the plasma frequency due only to the electron beam, and f_{0e} is the electron distribution function for the warm plasma electrons.

For mathematical simplicity, a resonance distribution function for the electrons is assumed, of the form

$$f_{0e}(v_z) = \frac{V_T}{\pi}\left(\frac{1}{v_z^2 + V_T^2}\right) \tag{A3}$$

where V_T is the average longitudinal thermal velocity.

The integral in (A2) can be computed by taking a contour in the upper half of the complex V_z plane with the result

$$\omega_{pe}^2 \int \frac{f_{0e}(v_z)dv_z}{(\omega - kv_z)^2} = \frac{\omega_{pe}^2}{(\omega - ikV_T)^2}$$

Thus (A2) becomes

$$K_{||}(\omega, k) = 1 - \frac{\omega_{pi}^2}{\omega^2} - \frac{\omega_{pe}^2}{(\omega - ikV_T)^2} \tag{A4}$$

An approximate solution for beam waves from (A1) is obtained by expanding around the beam velocity, $\omega \approx kV_0$. Equation (A1) is then rewritten by using the form $\omega - kV_0 = \delta\omega(k)$ where $\delta\omega \ll kV_0$. In this derivation $\delta\omega(k)$ is considered to be a small 'correction' to ω caused by the presence of the beam. It should be noted that the entire imaginary component of ω, which gives the growth rate, is contained in the $\delta\omega$ term. Since $\delta\omega$ is a small correction we can perform a Taylor series expansion of (A1) around $\omega = kV_0$ and obtain

$$\frac{\omega_{pb}^2}{\delta\omega^2} = K_{\|}(\omega = kV_0) + \delta\omega\left(\frac{\partial K_{\|}}{\partial\omega}\right)_{\omega=kV_0} \tag{A5}$$

Now in general, $K_{\|}(\omega = kV_0) = K_R + iK_I$, where the imaginary part of $K_{\|}$ arises from Landau damping. Instability occurs whenever a complex $\delta\omega$ with $Im(\delta\omega) < 0$ arises from (A5). As described in Briggs [1964] there are two basic types of instabilities that can occur. These are referred to as the reactive-medium instability and the resistive-medium instability.

The reactive-medium instability occurs if $V_0 \gg V_T$. In this case Landau damping can be neglected. This implies that K_I is vanishingly small and may be neglected in the solution of (A5). The solution obtained in this case is essentially the usual dispersion relation for Langmuir oscillations generated by a two-stream instability.

Of particular interest to this work is the resistive-medium instability. This instability is obtained from (A5) when $V_0 \approx 0(V_T)$ and $K_R > 0$. When V_0 is on the order of V_T, K_I cannot be neglected and Landau damping plays an important role in the solution of (A5). The novel feature in the resistive medium instability is that it requires Landau damping to obtain wave growth. If the final term is neglected in (A5) we obtain (using (A4))

$$\frac{\omega_{pb}^2}{\delta\omega^2} = K_{\|}(\omega = kV_0)$$

$$= 1 - \frac{\omega_{pi}^2}{\omega^2} - \frac{\omega_{pe}^2}{\omega^2\left(1 - i\dfrac{V_T}{V_0}\right)^2}$$

which can be written

$$\delta\omega^2 = \omega_{pb}^2\left[\frac{\omega^2\left(V^* - i2\dfrac{V_T}{V_0}\right)}{\omega^*\left(V^* - i2\dfrac{V_T}{V_0}\right) - \omega_{pe}^2}\right] \tag{A6}$$

where $V^* = 1 - (V_T/V_0)^2$, $\omega^* = \omega^2 - \omega_{pi}^2$.

Multiplying the top and bottom by the complex conjugate one obtains

$$\delta\omega^2 = \omega_{pb}^2[x + iy] \tag{A7}$$

where

$$x = \frac{\omega^2 V^*(\omega^* V^* - \omega_{pe}^2) + 4\omega^2\left(\dfrac{V_T}{V_0}\right)^2\omega^*}{(\omega^* V^* - \omega_{pe}^2)^2 + 4(\omega^*)^2\left(\dfrac{V_T}{V_0}\right)^2} \tag{A8}$$

and

$$y = \frac{2\omega^2\left(\dfrac{V_T}{V_0}\right)\omega_{pe}^2}{(\omega^* V^* - \omega_{pe}^2)^2 + 4(\omega^*)^2\left(\dfrac{V_T}{V_0}\right)^2} \tag{A9}$$

Thus $\delta\omega$ may be found by taking the complex square root of $\omega_{pb}^2[x + iy]$, so that

$$\delta\omega = \pm\omega_{pb}[x + iy]^{1/2} \tag{A10}$$

will be the solution for the resistive medium instability.

Acknowledgments. We wish to thank Roger R. Anderson and Dennis L. Gallagher for great assistance in the analysis of ISEE data, and Louis Frank for permission to use the LEPEDEA data from the ISEE 1 spacecraft. This research was supported by NASA through grants NGL-16-001-002 and NGL-16-001-043 from NASA Headquarters and contracts NAS5-20093, NAS5-26819, and NAS5-11074 with Goddard Space Flight Center and the Office of Naval Research. The LEPEDEA data reduction from the ISEE 1 instrument was performed through contract NAS5-26257 with Goddard Space Flight Center.

The Editor thanks B. Tsurutani and R. M. Thorne for their assistance in evaluating this paper.

REFERENCES

Anderson, R. R., G. K. Parks, T. E. Eastman, D. A. Gurnett, and L. A. Frank, Plasma waves associated with energetic particles streaming into the solar wind from the earth's bow shock, *J. Geophys. Res.*, *86*, 4493, 1981.

Brice, N., Fundamentals of very low frequency emission generation mechanisms, *J. Geophys. Res.*, *69*, 4515, 1964.

Briggs, R. J., *Electron-Stream Interaction With Plasmas*, *Res. Monogr. 29*, M.I.T. Press, Cambridge, Mass., 1964.

Burtis, W. J., and R. A. Helliwell, Banded chorus—A new type of VLF radiation observed in the magnetosphere by OGO 1 and OGO 3, *J. Geophys. Res.*, *74*, 3002, 1969.

Burtis, W. J., and R. A. Helliwell, Magnetospheric chorus: Occurrence patterns and normalized frequency, *Planet. Space Sci.*, *24*, 1007, 1976.

Burton, R. K., and R. E. Holzer, The origin and propagation of chorus in the outer magnetosphere, *J. Geophys. Res.*, *79*, 1014, 1974.

Dowden, R. L., Doppler-shifted cyclotron radiation from electrons: A theory of very low frequency emissions from the exosphere, *J. Geophys. Res.*, *67*, 1745, 1962.

Eastman, T. E., and L. A. Frank, Observations of high-speed plasma flow near the earth's magnetopause: Evidence for reconnection?, *J. Geophys. Res.*, *87*, 2187, 1982.

Frank, L. A., D. M. Yeager, H. D. Owens, K. L. Ackerson, and M. R. English, Quadrispherical LEPEDEAS for ISEE's-1 and -2 plasma measurements, *IEEE Trans. Geosci. Electron.*, *GE-16*, 221, 1978*a*.

Frank, L. A., K. L. Ackerson, R. J. DeCoster, and B. G. Burek, Three-dimensional plasma measurements within the earth's magnetosphere, *Space Sci. Rev.*, *22*, 739, 1978*b*.

Gurnett, D. A., and L. A. Frank, Ion acoustic waves in the solar wind, *J. Geophys. Res.*, *83*, 58, 1978.

Gurnett, D. A., and R. R. Shaw, Electromagnetic radiation trapped in the magnetosphere above the plasma frequency, *J. Geophys. Res.*, *78*, 8136, 1973.

Gurnett, D. A., F. L. Scarf, R. W. Fredricks, and E. J. Smith, The ISEE-1 and ISEE-2 plasma wave investigation, *IEEE Trans. Geosci. Electron.*, *GE-16*, 225, 1978.

Helliwell, R. A., *Whistlers and Related Ionospheric Phenomena*, Stanford University Press, Stanford, Calif., 1965.

Helliwell, R. A., A theory of discrete VLF emissions from the magnetosphere, *J. Geophys. Res.*, *72*, 4773, 1967.

Inan, U. S., and S. Tkalcevic, Nonlinear equations of motion for landau resonance interactions with a whistler mode wave, *J. Geophys. Res.*, *87*, 2363, 1982.

Kennel, C. F., and H. E. Petschek, Limit on stably trapped particle fluxes, *J. Geophys. Res.*, *71*, 1, 1966.

Kennel, C. F., and R. M. Thorne, Unstable growth of unducted whistlers propagating at an angle to the geomagnetic field, *J. Geophys. Res.*, *72*, 871, 1967.

Kennel, C. F., F. L. Scarf, F. V. Coroniti, R. W. Fredricks, D. A. Gurnett, and E. J. Smith, Correlated whistler and electron plasma oscillation bursts detected on ISEE 3, *Geophys. Res. Lett.*, *7*, 129, 1980.

Krall, N. A., and A. W. Trivelpiece, *Principles of Plasma Physics*, McGraw-Hill, New York, 1973.

Mikhailovskii, A. B., *Theory of Plasma Instabilities*, vol. 1, *Instabilities of a Homogeneous Plasma*, Consultants Bureau, New York, 1974.

Nunn, D., Wave particle interaction in electrostatic waves in an inhomogeneous medium, *J. Plasma Phys.*, *6*, 291, 1971.

Nunn, D., The sideband instability of electrostatic waves in an inhomogeneous medium, *Planet. Space Sci.*, *21*, 67, 1973.

Oliven, M. N., and D. A. Gurnett, Microburst phenomena, 3, An association between microbursts and VLF chorus, *J. Geophys. Res.*, *73*, 2355, 1968.

Reinleitner, L. A., Electrostatic bursts generated by electrons trapped in whistler mode chorus wave fields, Ph.D. dissertation, University of Iowa, Iowa City, 1982.

Reinleitner, L. A., D. A. Gurnett, and D. L. Gallagher, Chorus-related electrostatic bursts in the earth's outer magnetosphere, *Nature*, *295*, 46, 1982.

Rosenberg, T. J., R. A. Helliwell, and J. P. Katsufrakis, Electron precipitation associated with discrete very-low-frequency emissions, *J. Geophys. Res.*, *76*, 8445, 1971.

Russell, C. T., The ISEE 1 and 2 fluxgate magnetometers, *IEEE Trans. Geosci. Electron.*, *GE-16*, 239, 1978.

Stix, T. H., *The Theory of Plasma Waves*, McGraw-Hill, New York, 1962.

Thorne, R. M., and C. F. Kennel, Quasi-trapped VLF propagation in the outer magnetosphere, *J. Geophys. Res.*, *72*, 857, 1967.

Tkalcevic, S., Nonlinear longitudinal resonance interaction of energetic charged particles and VLF waves in the magnetosphere, Ph.D. dissertation, Stanford University, Stanford, Calif., 1982.

Van Allen, J. A., Dynamics, composition and origin of the geomagnetically-trapped corpuscular radiation, *Trans. Int. Astron. Union*, *11B*, 99, 1962.

(Received September 15, 1982;
revised December 21, 1982;
accepted December 22, 1982.)